Received: April 18, 2020. Revised: May 19, 2020. 

INASS

International Journal of
Intelligent Engineering & Systems

http://www.inass.org/

# Robust Sliding Mode Control with Five Sliding Surfaces of Five-Phase PMSG Based Variable Speed Wind Energy Conversion System

**Salah Eddine Rhaili[1]* Ahmed Abbou[1] Saloua Marhraoui[1] Rania Moutchou[1] Nezha El Hichami[1]**

[1]*Department of Electrical Engineering, Mohammadia School of Engineers, Mohammed V University in Rabat, Morocco*
* Corresponding author's Email: salah.rhaili@gmail.com

**Abstract:** The central thesis of this paper is the implementation of an optimized Sliding Mode Control to a high power multiphase permanent magnet synchronous generator based direct-driven Wind Energy Conversion System (WECS), in order to attain an optimal regime characteristic. The principle of proposed approach is to control the Rotational Speed Dynamic to follow the desired value during wind variations. Moreover, the controller is designed to ensure an effective regulation of 4 dynamic models of Direct & Quadrature axis current instead of the regular hysteresis control due to its disadvantages. In this context, the main challenge of this research with a view to ensure the system stability, is to design a controller in a way to guarantee the consistency between the input of inner loop (4 axis current regulation) and the output of outer loop (speed regulation), taking into account the risk of declined effectiveness of closed-loop due to disappearing relative changes in control periods between the cascaded loops. Furthermore, the grid supply is managed using the proposed sliding mode approach in order to guarantee a power injection with Unity Power Factor. On the other hand, a challenging matter of pure SMC can be summed up in the produced chattering phenomenon. In this work, this issue has been mitigated by implementing a new smooth continuous switching control. In order to examine the suggested approach robustness and responsiveness over other techniques, a detailed analysis has been carried out under hard and random wind speed variations. The stability of improved SMC is verified using Lyapunov stability theory by taking into account system uncertainties to guarantee more efficacy. The suggested SMC is compared to a classical PI controller. The study results exhibit the excellent performance with high robustness of the improved SMC, by improving the system efficiency to 91,14%, compared to the PI with the ratio of 86,2%.

**Keywords:** MPPT, Sliding mode control, Nonlinear control, Lyapunov stability, Chattering elimination, Permanent magnet generator, Five-phase PMSG, Power extraction, Variable speed wind turbine, Pitch control, Grid control.

## 1. Introduction

In practical terms, (WECS) exploits various kinds of machines as generators. By reason of its expensive and complicated control systems, the induction generators (DFIGs) have been replaced by permanent magnet synchronous generators (PMSGs) [1],what gives the WECS more dependability, better accuracy and increased performance [2]. A PMSG has the advantage of allowing the direct coupling of mechanical system and rotor, which provides an important factor in reducing wind turbines installation, management and maintenance costs, especially at high power capacities as offshore systems [3].Reasoning from this fact, a multiphase PMSG became more attractive to be installed as wind turbine generator, due to its significant advantages as fault-tolerance ability, increased power, reduced component costs, reduced DC bus ripple, reduced operating noise, more efficient use of cable cross-sectional area and easier integration. In addition, the Multiphase PMSGs offer the benefit of creating high torque output because of the huge magnetic flux density and efficacy [4-6]. On the other hand, wind

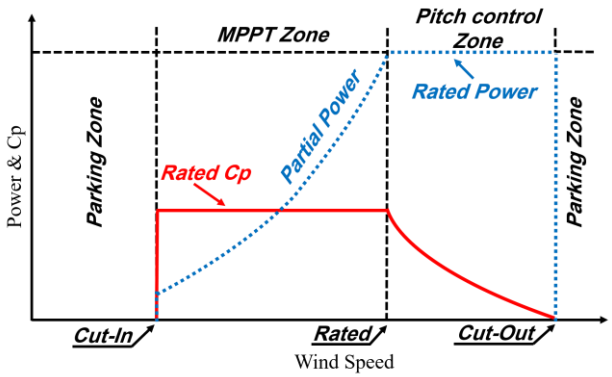


Figure. 1 Operation zones of wind turbine

turbine can be classified into two models depending on the operating mode, variable and fixed speed systems. By analyzing these two models. It can be deduced that the variable speed type is more flexible and polyvalent compared to the fixed speed kind, by elevating energy quality, lowering mechanical stress and enhancing the generated power up to ten percent [7]. There are three operational regions for the variable wind turbine (VSWT) as Fig. 1 illustrates. At the MPPT zone, a torque control is used in order to control the system to track its maximum power , but when the wind speed gets above the rated level, a pitch control is necessary to keep the system at its rated dynamic.

In research field, many publications have proposed different algorithms to track and maintain the maximum power extraction [8, 9]. However, the capability to attain an adequate performance was a challenging topic, because of the capricious character of wind. The most famous control of (VSWT) is the field oriented control, which can be processed by using a PI controllers [10, 11].The main deficiency of this method is the adjustment of PI gains. For this reason, the efficiency is always rely on the correct identification of system parameters. To resolve this issue, other methods have been proposed as Direct Torque Control and Direct Power Control [12], Which have the ability to reduce the necessity of wind turbine parameters, and improve the performance as [13, 14] proved. Yet, the major disadvantage of these kind of strategies is the switching frequency of Pulse width modulated converters, which fluctuates during input variations. Moreover, the system experiences vital torque and/or power ripples during the steady state. On the other hand, many researches have been tried hysteresis controller to regulate the PMSG current. However, the major disadvantage of this control, among others, is injecting high-frequency harmonics into the system current, as [15] demonstrates. As a result of the bounded accomplishments of classic vector control and direct control techniques, modern nonlinear approaches can be used to enhance WECS performance. Various nonlinear methods have been proposed to improve control robustness, as adaptive control [16, 17], anyhow, when the adaptive control is being constructed, multiple design parameters is occurred and required to be determined. Even so, it affects the controlled system stabilization and performance. Authors in [18] proposed a PMSG backstepping control, the results demonstrate the effectiveness of the chosen control. Yet, the response time still has a certain tracking delay. Besides, using this technique, measuring all state variables is necessary, or a nonlinear observer is required. In a similar manner, [19] has discussed a five-phase PMSG speed control using fuzzy logic algorithm, and compared it to a classic PI under open phase fault, to demonstrate the superiority of nonlinear controls. Nevertheless, fuzzy logic depends on the test and failure for enhancement. Likewise, it can sometimes be inaccurate. Moreover, [20] designed a new MPPT controller based on neural networks strategy. Despite the great performance, operating ANN needs a lot of time for training with enormous data. Besides, one of the suggested algorithms to control nonlinear systems as wind turbine is the sliding mode control (SMC). The SMC has shown a promising result to achieve a high degree of reliability, accuracy and stability, with a major flexibility during parameters variations [21]. Pure SMC technique faces the chattering appearance. Therefore, several composite SMC architectures have been built in combination with other approaches, as Fuzzy-sliding mode [22]. Despite the ability of chattering reduction, these mixed methods necessitate complex application process, especially at high power capacities systems as the extended version of PMSG with several control loops. Within this framework , the main target of this paper, on the one hand, is to produce an appropriate design of VSWT consists of a five phase PMSG instead of the conventional three phase PMSG due to its various aforementioned advantages , and on the other hand, improve and enhance the effectiveness of proposed system, by involving an optimized sliding mode control that supervises the entire system of wind turbine and the connected grid supply, due to its high degree of robustness, ability of reducing the dynamic response time, and most of all its exploitation simplicity. Moreover, the proposed robust SMC algorithm consist of an enhancement method based on a new smooth switching function with integral component so as to mitigate the chattering phenomenon and reduce the energy loss, thereby, improve the efficiency and accuracy in this work. Moreover, the structure of optimized SMC is

replacing hysteresis current control due to its above-mentioned drawbacks, in order to manage the five-phase current smoothly and get a balanced signal.

The contribution made over this work can outlined as: Developing an accurate model of WECS based on high power five-phase PMSG. Pitch control has been implemented in order to hold the power extraction at its rated level, and guarantee (WT) safety. Establishing an optimized sliding mode control law to manage both MSC and GSC, taking into account system reaction against dynamic turbulences and external elements variations. Lyapunov stability condition is involved in order to prove the proposed approach stability. PI control has been applied and compared to the studied SMC technique. The results analysis displays an improvement in the system performance using SMC, with higher efficacy ratio of 91,14%, compared to the PI efficiency of 86,2%.

This paper is arranged in six sections: After the first section that gives a general introduction, section 2 comes to exhibit the studied system modeling. Then, section 3 describes the pitch angle control and clarify the machine side sliding mode control laws with an inclusive analysis based on the stability approach. Section 4 provides the grid side command by applying the proposed sliding mode control-based Voltage Oriented Control. Thereafter, section 5 reveals the simulation results and interpretations. Finally, section 6 is reserved for a summarized conclusion.

## 2. Wind turbine and generator modelling

### 2.1 Turbine Model

The study is carried out by using a variable speed wind turbine (VSWT) with a variable pitch, a five-phase permanent magnet generator coupled to the grid via two back-to-back converters and RL filter. The 5-phase rectifier has a role of ensuring a maximum power tracking, However, the 3-phase inverter controls the DC-link voltage to keep its invariable state, and holds the grid unity power factor. The (VSWT) transforms the captured wind power to a mechanical power, which can be expressed as:

$$P_{tr} = \frac{1}{2}.\rho S.V_w^3.C_p(\beta\lambda) \quad (1)$$

The produced mechanical torque is:

$$T_m = \frac{P_m}{\omega_m} \quad (2)$$

### 2.2 Modeling of five phase PMSG

Application of an extended Park's Transformation to the five-coordinate of five-phase PMSG dynamic model gives the direct and quadrature axis voltages in synchronous rotating frame as follows [23, 24]:

$$\begin{cases} V_{d1} = R_s i_{d1} + L_{d1}\frac{di_{d1}}{dt} - \omega_e L_q i_{q1} \\ V_{q1} = R_s i_{q1} + L_{q1}\frac{di_{q1}}{dt} + \omega_e L_d i_{d1} + \omega_e \psi_{pm} \\ V_{d2} = R_s i_{d2} + L_{d2}\frac{di_{d2}}{dt} - 3\omega_e L_q i_{q2} \\ V_{q2} = R_s i_{q2} + L_{q2}\frac{di_{q2}}{dt} + 3\omega_e L_d i_{d2} \end{cases} \quad (3)$$

When the PMSG has a uniform air gap, then $L_d = L_q = L_s$.

The electromagnetic torque of 5-phase PMSG can be represented if $i_{d1}$, $i_{d2}$, and $i_{q2}$ are driven to zero as:

$$T_e = \frac{5}{2}p\psi_{pm}i_{q1} \quad (4)$$

The mechanical equation of the wind turbine system can be formulated as:

$$\frac{d\omega_m}{dt} = \frac{T_e}{J} - \frac{T_m}{J} - \frac{B\omega_m}{J} \quad (5)$$

## 3. Machine side converter sliding mode control

Fig. 3 demonstrates the overall control scheme. The main purpose of machine side control is to maximize the extracted power (Pm) of (VSWT) under wind variations. To meet this target, the five-phase PMSG must reach its optimum speed, by forcing the turbine to operates at maximum power coefficient ($C_p$). Thereby, a critical factor named tip-

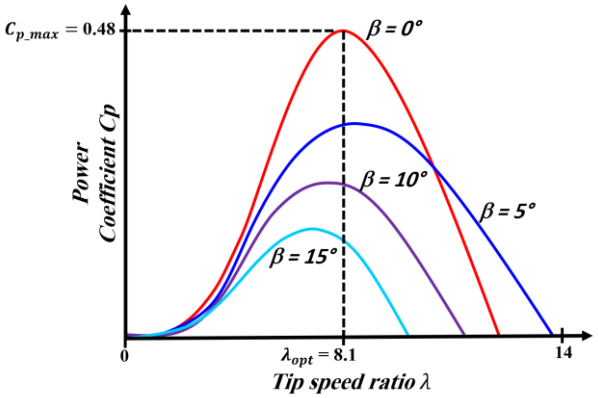


Figure. 2 Power coefficient as function of TSR (λ) and (β)

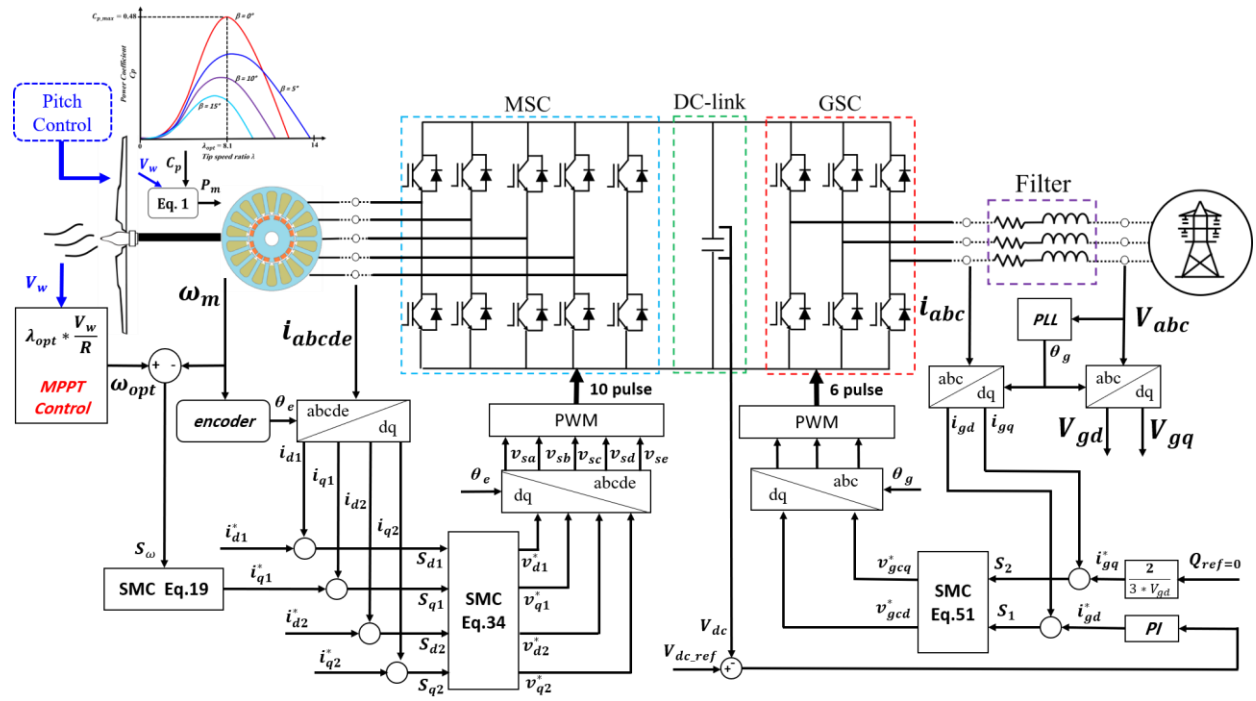


Figure. 3 Overall control architecture

speed ratio (TSR) is kept at its rated value ( $\lambda_{opt}$ = 8.1) when the system is working at the MPPT zone as Fig. 2 mentions about the relation between ($C_p$) & (TSR). The optimum speed of PMSG can be expressed by:

$$\omega_{m\_opt} = \lambda_{opt}.\frac{V_w}{R} \quad (6)$$

Accordingly, the optimal generated power of wind turbine can be written as:

$$P_{turbine\_max} = \frac{1}{2}.\rho.S.\left(R.\frac{\omega_{m\_opt}}{\lambda_{opt}}\right)^3.C_{p\_max} \quad (7)$$

When the (WT) gets above the rated wind speed region, the system uses a pitch control as a means to hold the power extraction at its rated level, to guarantee the (WT) protection and safety. There are various mechanisms to carry out the pitch control. Fig. 4 represents the aerodynamic technique of first order system applied to achieve a satisfying pitch angle adjustment. The controller processes the speed variations bunch of times and produce a reference pitch angle, then the system runs the servo in order to reduce the pitch angle error.

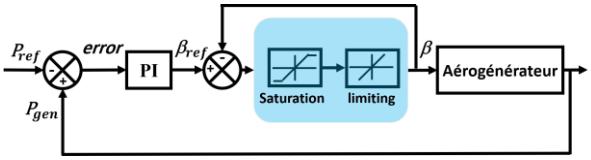


Figure. 4 Pitch angle control

To apply the MPPT of wind turbine in MSC, the Sliding Mode approach has been involved, with two cascaded control loops, due to its effectiveness, simplicity, and the great accuracy contrary to other approaches. The outer loop sets and supervises the generator speed, and creates a reference of the first current component ($i_{q1}^*$) of quadrature axis based on Eqs. (4) and (5), that relate it to the electromagnetic torque and the generated speed. Whilst, the inner loop commands the 4 direct and quadrature axis currents of generator to follow their references. Furthermore, it ensures the Maximum Torque Per Ampere (MTPA) Control [25]. The main challenge of this study is to ensure the consistency between the output of outer loop and the input of inner loop of SMC controller.

SMC is one of the most nonlinear clever and resilient strategies to monitor the performance of systems due to its insensitivity to parameters variations and external disturbances. The presented SMC surpasses the chattering phenomenon using the enhanced switching control law and fixes the reaching phase unsteadiness issue. Moreover, the controller improves the generated energy through following the rated PMSG speed during wind alteration. In the main, sliding mode control has three designing steps. First one is to choose the sliding surface in accordance with the developed 5-phase PMSG architecture, in order to design the closed-loop dynamic inside the variable state space. Next, the convergence condition is required to sustain the system control capability. Finally, the control

strategy is created in a way to lead the system paths into the sliding surface and remains there [26-27]. The sliding surface can be defined using time-varying equation as [27]:

$$S(X,t) = \left(\frac{d}{dt} + \xi\right)^{m-1} e_x(t) \quad (8)$$

$(\xi)$ is a positive constant that identifies the declivity of the sliding surfaces, *(m)* is the decided order degree, $(e_x)$ is the error between $x_{ref}$ & $x$ ( $x_{ref}$ is the desired signal, and $x$ is the state variable).

The switching function S(t) has been chosen for ($m$=1) as the tracking error e(t):

$$S(X,t) = e(t) = x_{ref} - x \quad (9)$$

The main dilemma of following the reference vector is summarized in keeping the desired and the generated signals at the same value permanently. By other means, the objective is achieved if:

$$\lim_{t\to\infty} e = \lim_{t\to\infty} x_{ref} - x = 0 \quad (10)$$

Thus, the convergence condition to make the sliding movement is expressed by the following terms:

$$S(X,t) = \dot{S}(X,t) = 0 \quad (11)$$

Furthermore, in order to keep the switching nearby the sliding mode surface, an equivalent SMC formula u(t) is developed as the addition of two expressions:

$$u(t) = u_{eq}(t) + u_n(t) \quad (12)$$

$u_{eq}(t)$ is the state-continuous equivalent control, $u_n(t)$ expresses the switching effort which can be specified as:

$$u_n = -\delta_n . Smooth(S_n) \quad (13)$$

$\delta_n$ is the positive gain of SMC, ***Smooth*** is the continuous mathematical function of $C^1$ class, which replaces the ordinary discontinuous ***Sign*** function in order to reduce the chattering phenomenon:

$$Smooth(S_n) = \frac{\mathrm{S(t)}}{\|\mathrm{S(t)}\|+\gamma} \quad (14)$$

In the machine side control, 5 sliding surfaces have been fixed: $S_\omega, S_{d1}, S_{q1}, S_{d2}$ and $S_{q2}$.

The first one ($S_\omega$) is related to the speed error as:

$$S_\omega(t) = \left[\omega_{m\_opt}(t) - \omega_m(t)\right] \quad (15)$$

By taking time derivative of $S_\omega(t)$, then:

$$\dot{S}_\omega = \dot{\omega}_{m\_opt} - \dot{\omega}_m \quad (16)$$

Now, merging Eqs. (4) and (5), a relation between rotor speed variation and quadrature axis current component is revealed:

$$J\dot{\omega}_m = \frac{5}{2} p\psi i_{q1} - T_m - B\omega_m \quad (17)$$

Eq. (16) can be reformulated using Eq. (17) as:

$$\dot{S}_\omega = \dot{\omega}_{m\_opt} - \frac{1}{\mathrm{J}}\left(\frac{5}{2} p\psi i_{q1} - T_m - B\omega_m\right) \quad (18)$$

When the sliding surface is reached, Eqs. (18) and (13) are equalized, then the velocity control equation can be developed as:

$$i_{q1}^* = A^{-1}[J\dot{\omega}_{m\_opt} + T_m + B\omega_m + J\delta_\omega . Smooth(S_\omega)] \quad (19)$$

With $A = \frac{5}{2} p\psi_{pm}$

Besides, with the objective of controlling the direct and quadrature current components, the sliding surfaces are formulated using Eq. (9) as:

$$S_{d,\mathrm{i}}(t) = \left[i_{d,\mathrm{i}}^*(t) - i_{d,\mathrm{i}}(t)\right] ; \{i = 1,2\} \quad (20)$$

$$S_{q,\mathrm{i}}(t) = \left[i_{q,\mathrm{i}}^*(t) - i_{q,\mathrm{i}}(t)\right]; \{i = 1,2\} \quad (21)$$

Applying time derivative to $S_{d1}, S_{q1}, S_{d2}$ and $S_{q2}$ from Eqs. (20) and (21), the resulting equations are:

$$\frac{d}{dt} S_{d1\_2} = \frac{d}{dt} i_{d1\_2}^*(t) - \frac{d}{dt} i_{d1\_2}(t) \quad (22)$$

$$\frac{d}{dt} S_{q1\_2} = \frac{d}{dt} i_{q1\_2}^*(t) - \frac{d}{dt} i_{q1\_2}(t) \quad (23)$$

Using Eq. (3), PMSG voltages can be expressed as:

$$\frac{di_{d1}}{dt} = -\frac{R_s}{L_s} i_{d1} + \omega_e i_{q1} + \frac{1}{L_s} V_{d1} \quad (24)$$

$$\frac{di_{q1}}{dt} = -\frac{R_s}{L_s} i_{q1} - \omega_e i_{d1} - \frac{\psi_{pm}\omega_e}{L_s} + \frac{1}{L_s} V_{q1} \quad (25)$$

$$\frac{di_{d2}}{dt} = -\frac{R_s}{L_s} i_{d2} + 3\omega_e i_{q2} + \frac{1}{L_s} V_{d2} \quad (26)$$

$$\frac{di_{q2}}{dt} = -\frac{R_s}{L_s} i_{q2} - 3\omega_e i_{d2} + \frac{1}{L_s} V_{q2} \quad (27)$$

By replacing Eqs. (24), (25), (26) and (27) in Eqs. (22) and (23) successively, the produced equations are:

$$\frac{d}{dt}S_{d1} = \frac{d}{dt}i_{d1}^{*} - \frac{1}{L_s}\left(-R_s i_{d1} + L_s\omega_e i_{q1} + V_{d1}\right) \quad (28)$$

$$\frac{d}{dt}S_{q1} = \frac{d}{dt}i_{q1}^{*} - \frac{1}{L_s}\left(-R_s i_{q1} - L_s\omega_e i_{d1} - \psi_{pm}\omega_e + V_{q1}\right) \quad (29)$$

$$\frac{d}{dt}S_{d2} = \frac{d}{dt}i_{d2}^{*} - \frac{1}{L_s}\left(-R_s i_{d2} + 3L_s\omega_e i_{q2} + V_{d2}\right) \quad (30)$$

$$\frac{d}{dt}S_{q2} = \frac{d}{dt}i_{q2}^{*} - \frac{1}{L_s}\left(-R_s i_{q2} - 3L_s\omega_e i_{d2} + V_{q2}\right) \quad (31)$$

Denoting the *dq12-axis* control laws:

$$v_{d,i}^{*} = v_{d,\mathrm{i}\_eq} + v_{d,\mathrm{i}\_n}\,;\{i = 1{,}2\} \quad (32)$$

$$v_{q,\mathrm{i}}^{*} = v_{q,\mathrm{i}\_eq} + v_{q,\mathrm{i}\_n}\,;\{i = 1{,}2\} \quad (33)$$

Where $v_{\mathrm{i}\_eq}$ is the equivalent control, and $v_{\mathrm{i}\_n}(\mathrm{t})$ is the switching control.

After Merging Eqs. (28), (29), (30), and (31) into Eqs. (32) and (33), the voltages control equations are obtained as:

$$\begin{cases} v_{d1}^{*} = R_s i_{d1} - \omega_e L_s i_{q1} + L_s\frac{d}{dt}i_{d1}^{*} \\ \qquad +L_s\delta_{d1}.Smooth(S_{d1}) \\ v_{q1}^{*} = R_s i_{q1} + \omega_e L_s i_{d1} + \omega_e\psi_{pm} + L_s\frac{d}{dt}i_{q1}^{*} \\ \qquad +L_s\delta_{q1}.Smooth\left(S_{q1}\right) \\ v_{d2}^{*} = R_s i_{d2} - 3\omega_e L_s i_{q2} + L_s\frac{d}{dt}i_{d2}^{*} \\ \qquad +L_s\delta_{d2}.Smooth(S_{d2}) \\ v_{q2}^{*} = R_s i_{q2} + 3\omega_e L_s i_{d2} + L_s\frac{d}{dt}i_{q2}^{*} \\ \qquad +L_s\delta_{q2}.Smooth\left(S_{q2}\right) \end{cases} \quad (34)$$

Where the constants $\delta_{d1}$ >0, $\delta_{q1}$ >0, $\delta_{d2}$ >0, $\delta_{q2}$ >0
Now, to prove the global asymptotic stability condition of proposed SMC using the designed dynamic rules in Eqs. (19) and (34), the Lyapunov function candidate is elected as:

$$\Gamma_{MSC} = \frac{1}{2}S_\omega^2 + \frac{1}{2}S_{d1}^2 + \frac{1}{2}S_{q1}^2 + \frac{1}{2}S_{d2}^2 + \frac{1}{2}S_{q2}^2 \quad (35)$$

The Lyapunov method for stability presupposes that the sliding mode is achieved **iff**: $\frac{d\,\Gamma_{MSC}}{dt} < 0$

Hence, taking the time derivative of $\Gamma_{MSC}$, the obtained equation is:

$$\frac{d\,\Gamma_{MSC}}{dt} = S_\omega\frac{dS_\omega}{dt} + S_{d1}\frac{dS_{d1}}{dt} + S_{q1}\frac{dS_{q1}}{dt} + S_{d2}\frac{dS_{d2}}{dt} + S_{q2}\frac{dS_{q2}}{dt} \quad (36)$$

Using Eqs. (18), (24), (25), (26) and (27), then Eq. (36) can be reformulated as:

$$\frac{d\,\Gamma_{MSC}}{dt} = S_\omega.\left[\dot{\omega}_{m\_opt} - \frac{1}{\mathrm{J}}(A.i_{q1} - T_m - B\omega_m)\right] + S_{d1}\left[\frac{d}{dt}i_{d1}^{*} - \frac{1}{L_s}\left(-R_s i_{d1} + L_s\omega_e i_{q1} + V_{d1}\right)\right] + S_{q1}\left[\frac{d}{dt}i_{q1}^{*} - \frac{1}{L_s}\left(-R_s i_{q1} - L_s\omega_e i_{d1} - \psi_{pm}\omega_e + V_{q1}\right)\right] + S_{d2}\left[\frac{d}{dt}i_{d2}^{*} - \frac{1}{L_s}\left(-R_s i_{d2} + 3L_s\omega_e i_{q2} + V_{d2}\right)\right] + S_{q2}\left[\frac{d}{dt}i_{q2}^{*} - \frac{1}{L_s}\left(-R_s i_{q2} - 3L_s\omega_e i_{d2} + V_{q2}\right)\right] \quad (37)$$

Taking into account unmodelled dynamics, the system uncertainties are considered as $X = \hat{X} + \Delta X$, with $\hat{X}$ is the formal value, and $\Delta X$ is a bounded disturbance [28]. Using Eqs. (19) and (34), it becomes:

$$\frac{\mathrm{d}\,\Gamma_{\mathrm{MSC}}}{\mathrm{dt}} = \left\{\mathrm{S}_\omega.\left[\underbrace{\frac{1}{\mathrm{J}}\left(\Delta\mathrm{J}\dot{\omega}_{\mathrm{m\_opt}} + \Delta\mathrm{T}_\mathrm{m} + \Delta\mathrm{B}\omega_\mathrm{m} - \Delta\mathrm{A}.\,\mathrm{i}_{\mathrm{q1}}\right)}_{\mathrm{D1}} - \delta_\omega.\mathrm{Smooth}(\mathrm{S}_\omega)\right] + \mathrm{S}_{\mathrm{d1}}.\left[\underbrace{\frac{1}{\mathrm{L_s}}\left(\Delta\mathrm{L_s}\frac{\mathrm{d}}{\mathrm{dt}}\mathrm{i}_{\mathrm{d1}}^{*} + \Delta\mathrm{R_s}\mathrm{i_{d1}} - \Delta\mathrm{L_s}\omega_\mathrm{e}\mathrm{i_{q1}}\right)}_{\mathrm{D2}} - \delta_{\mathrm{d1}}.\mathrm{Smooth}(\mathrm{S_{d1}})\right] + \mathrm{S}_{\mathrm{q1}}.\left[\underbrace{\frac{1}{\mathrm{L_s}}\left(\Delta\mathrm{L_s}\frac{\mathrm{d}}{\mathrm{dt}}\mathrm{i}_{\mathrm{q1}}^{*} + \Delta\mathrm{R_s}\mathrm{i_{q1}} + \Delta\mathrm{L_s}\omega_\mathrm{e}\mathrm{i_{d1}}\right)}_{\mathrm{D3}} - \delta_{\mathrm{q1}}.\mathrm{Smooth}(\mathrm{S_{q1}})\right] + \mathrm{S}_{\mathrm{d2}}.\left[\underbrace{\frac{1}{\mathrm{L_s}}\left(\Delta\mathrm{L_s}\frac{\mathrm{d}}{\mathrm{dt}}\mathrm{i}_{\mathrm{d2}}^{*} + \Delta\mathrm{R_s}\mathrm{i_{d2}} - 3\Delta\mathrm{L_s}\omega_\mathrm{e}\mathrm{i_{q2}}\right)}_{\mathrm{D4}} -$$

$$\delta_{d2}.\mathrm{Smooth}(\mathrm{S_{d2}})\Big] +$$

$$\mathrm{S_{q2}}.\Bigg[\underbrace{\frac{1}{\mathrm{L_s}}\Big(\Delta\mathrm{L_s}\frac{\mathrm{d}}{\mathrm{dt}}\mathrm{i}^*_{\mathrm{q2}} + \Delta\mathrm{R_s}\mathrm{i_{q2}} + 3\Delta\mathrm{L_s}\omega_\mathrm{e}\mathrm{i_{d2}}\Big)}_{\mathrm{D5}} -$$

$$\delta_{\mathrm{q2}}.\mathrm{Smooth}(\mathrm{S_{q2}})\Bigg]\Bigg\} \quad (38)$$

$$\frac{d\,\Gamma_{MSC}}{dt} = -\delta_\omega.|S_\omega| + S_\omega.D1 - \delta_{d1}.|S_{d1}| + S_{d1}.D2 - \delta_{q1}.|S_{q1}| + S_{q1}D3 - \delta_{d2}.|S_{d2}| + S_{d2}D4 - \delta_{q2}.|S_{q2}| + S_{q2}D5 \quad (39)$$

For $\delta_\omega > |D1|, \delta_{d1} > |D2|, \delta_{q1} > |D3|, \delta_{d2} > |D4|, \delta_{q2} > |D5|$; $\frac{d\,\Gamma_{MSC}}{dt} < 0$

Therefore, Lyapunov condition is verified and the main objective of proposed control is achieved.

## 4. Grid side converter control

The grid side converter has the role of controlling the power injection toward the grid, by applying an improved Sliding Mode Control based voltage-oriented control (VOC) [29]. The schematic design of main control comes with two control loops, an outer loop with the aim of keeping the DC-link voltage at a constant reference value, and an inner loop that adjust the *dq-axis* current to guarantee the grid UPF. The detailed scheme of the considered grid side control is illustrated in Fig.3. The GSC equations in the dq-axis reference frame, with the grid voltage vector, can be presented as:

$$\begin{cases} V_{gcd} = R_g i_{gd} + L_g \frac{di_{gd}}{dt} - L_g\omega_g i_{gq} + V_{gd} \\ V_{gcq} = R_g i_{gq} + L_g \frac{di_{gd}}{dt} + L_g\omega_g i_{gd} + 0 \end{cases} \quad (40)$$

The active and reactive power can be stated as:

$$P = \frac{3}{2}V_{gd}i_{gd} \quad (41)$$

$$Q = \frac{3}{2}V_{gd}i_{gq} \quad (42)$$

The voltage equations from Eq. (40) can be reformulated to be as:

$$\frac{di_{gd}}{dt} = \frac{1}{L_g}\left(-R_g i_{gd} + L_g\omega_g i_{gq} - V_{gd} + V_{gcd}\right) \quad (43)$$

$$\frac{di_{gq}}{dt} = \frac{1}{L_g}\left(-R_g i_{gd} - L_g\omega_g i_{gd} + V_{gcq}\right) \quad (44)$$

The following sliding surfaces $S_1$ and $S_2$ have been chosen to control grid current components $i_{gd}$, $i_{gq}$ :

$$S_1 = i^*_{gd} - i_{gd} \quad (45)$$

$$S_2 = i^*_{gq} - i_{gq} \quad (46)$$

Where, $i^*_{gd}$ , $i^*_{gq}$ are the desired dq-axis grid currents. Thus, the time derivatives of Eqs. (45) and (46) can be calculated using Eqs. (43) and (44) as:

$$\frac{dS_1}{dt} = \frac{di^*_{gd}}{dt} - \frac{1}{L_g}\left(-R_g i_{gd} + L_g\omega_g i_{gq} - V_{gd} + V_{gcd}\right) \quad (47)$$

$$\frac{dS_2}{dt} = \frac{di^*_{gq}}{dt} - \frac{1}{L_g}\left(-R_g i_{gq} - L_g\omega_g i_{gd} + V_{gcq}\right) \quad (48)$$

Denoting the dq12-axis control laws:

$$v^*_{gcd} = v_{gcd\_eq} + v_{gcd\_n} \quad (49)$$

$$v^*_{gcq} = v_{gcq\_eq} + v_{gcq\_n} \quad (50)$$

After Merging Eqs. (47) and (48) into Eqs. (49) and (50), the control equations are obtained as:

$$\begin{cases} v^*_{gcd} = L_g \frac{di^*_{gd}}{dt} + R_g i_{gd} - L_g\omega_g i_{gq} + V_{gd} \\ \qquad +\delta_1.L_g Smooth(S_1) \\ v^*_{gcq} = L_g \frac{di^*_{gq}}{dt} + R_g i_{gq} + L_g\omega_g i_{gd} \\ \qquad +\delta_2.L_g Smooth(S_2) \end{cases} \quad (51)$$

Where the constants $\delta_1 > 0$ and $\delta_2 > 0$

To prove the global asymptotic stability condition of the grid SMC using the designed dynamic rules in Eq. (51), Lyapunov's stability function is elected as:

$$\Gamma_{GSC} = \frac{1}{2}S_1^2 + \frac{1}{2}S_2^2 \quad (52)$$

according to the Lyapunov theory for stability, the sliding mode is achieved **iff:** $\frac{d}{dt}\Gamma_{GSC} < 0$

Hence, taking the time derivative of $\Gamma_{GSC}$, the obtained equation is:

$$\frac{d}{dt}\Gamma_{GSC} = S_1\frac{dS_1}{dt} + S_2\frac{dS_2}{dt} \quad (53)$$

Therefore, using Eqs. (47), (48), and (51), then Eq. (53) can be reformulated as:

$$\frac{d}{dt}\Gamma_{GSC} = -\delta_1 S_1.Smooth(S_1) - \delta_2 S_2 Smooth(S_2) \quad (54)$$

Thus, $\frac{d}{dt}\Gamma_{GSC} = -\delta_1|S_1| - \delta_2|S_2|$ (55)

For $\delta_1 > 0$ and $\delta_2 > 0$ ; $\frac{d}{dt}\Gamma_{GSC} < 0$

Therefore, the Lyapunov condition is verified and the main objective of proposed control is achieved.

## 5. Simulation results

To examine the effectiveness of proposed SMC based Maximum power point tracking of wind turbine, a WECS with a large scale five-phase PMSG has been performed under hard and random variations of wind speed. Moreover, the connected grid has been considered and controlled using SMC based VOC in order to operate the grid side at Unity Power Factor. Then, a PI control has been applied and compared to the studied SMC technique, to confirm the proposed mechanism robustness. The voltage phase locked loop (PLL) is engaged in the system to guarantee the synchronization with the electric network. Digital simulation study of the general structure with the pitch angle control has been carried out through Matlab/Simulink platform. The used parameters are documented in Table 1, by considering a healthy network conditions. The sliding mode control of MSC and GSC gains are selected in way to fulfill an optimum efficiency and accuracy regardless the system uncertainties and disturbance.

The wind speed time profile is explored in Fig. 5, with a rated wind velocity of $V_n$=11m/s. As can be seen in Fig. 6–7, when the system works under the rated speed, the pitch controller is disabled so the pitch angle is maintained at (0°), and (TSR) is kept at its optimal rate ($\lambda_{opt}$=8.1), then the power coefficient of wind turbine is oscillating around its maximum value (0.48). Nevertheless, once the rated wind speed is crossed ($V_w > V_n$), the pitch angle rises and the power coefficient drops ($C_p < C_{pmax}$) in order to keep the generator at the safe operation zone, thus, the generated power is sustained at a maximum value of

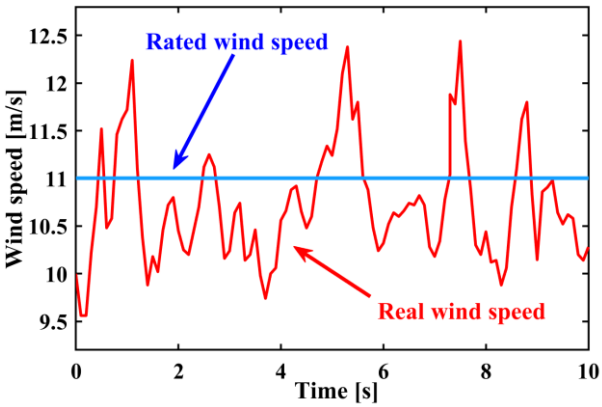


Figure. 5 Wind speed

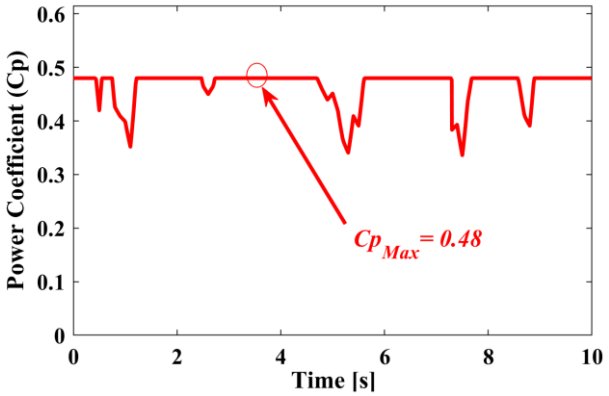


Figure. 6 Power coefficient

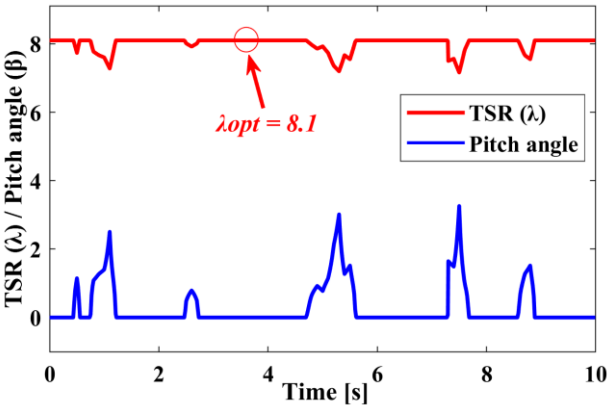


Figure. 7 Pitch angle (β) and Tip speed ratio (λ)

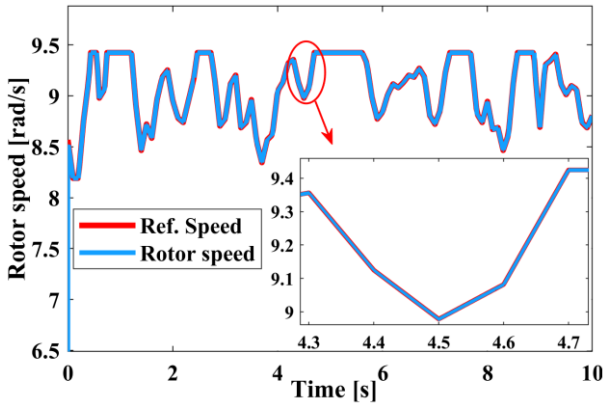


Figure. 8 Generator speed

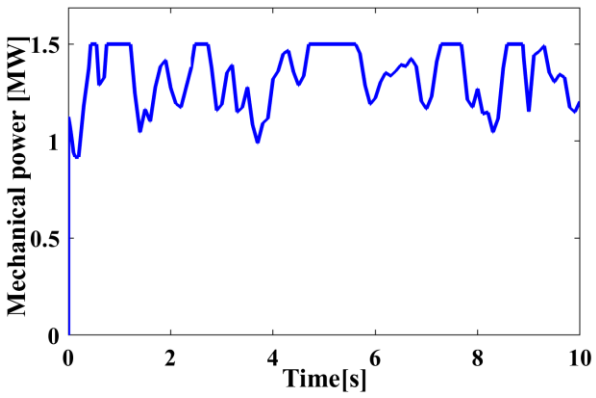


Figure. 9 Mechanical power

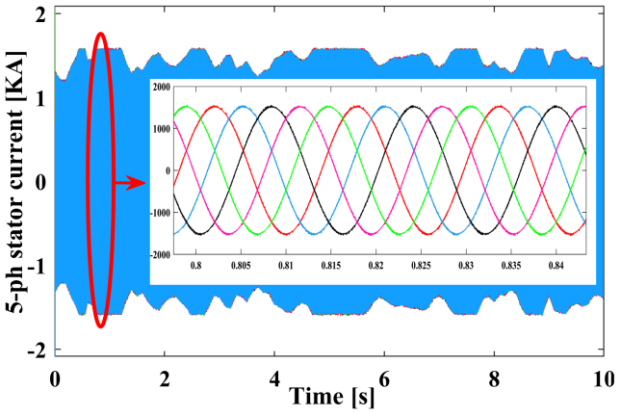


Figure. 10 Five-phase stator current

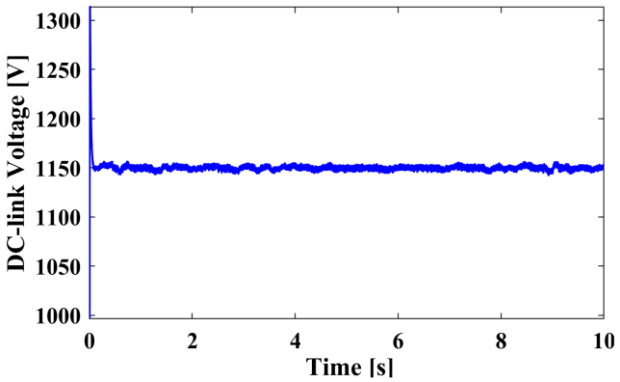


Figure. 11 DC-link voltage

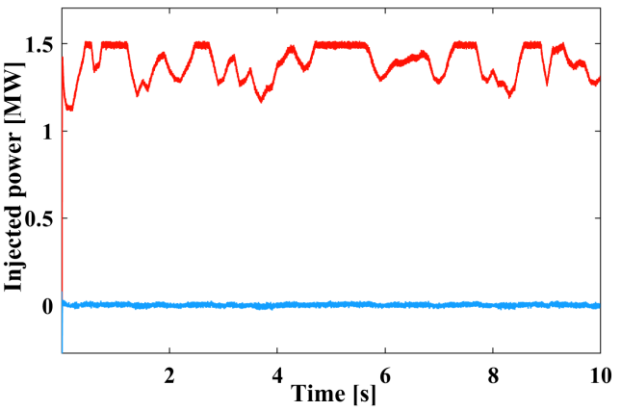


Figure. 12 Injected power into the grid

(1.5MW). Moreover, it is obvious from Fig. 8-10 that the angular velocity, the output power and five-phase PMSG current paths are responding accurately to the wind speed variations time. Additionally, the PMSG rotational speed is following its reference rapidly with exactness, using the proposed SMC approach. Besides, Table 2 presents the MSC current and voltage ripples, the produced five-phase currents are balanced with a smooth response. Hence, the system gives an appropriate performance.

The GSC performance under the SMC is verified. From Fig. 13, the grid voltage is in phase with the current and both have smooth and steady signals, since the reactive power is set to zero by controlling the q-axis current to zero based on Eq. (42). Thus, the UPF is achieved independently to the wind speed variations. Furthermore, according to Eq. (41), it can be reported that the proposed SMC is driving the injected active power into the grid to follow accurately the wind path by controlling the d-axis current as Fig. 12 proves. On the other hand, Fig. 11 demonstrates that the dc-link voltage is adjusted to settle around a continuous reference of (1150 V).

To verify the superiority of proposed SMC over conventional techniques, the improved SMC and a classical PI have been examined using ramp profile of wind speed. Fig. 14 proves that the PMSG rotational speed is following its reference faster with an average time of (0.1s) to reach the primary optimum value using SMC, while the PI controller needs (0.79s). Thus, the designed SMC provides better achievement in term of dynamic response. Addedly, Table 2 emphasizes the claims, with smaller oscillations and reduced switching losses using the developed SMC. Moreover, WECS efficiency of tracking the maximum power during wind variations has been established using the following equations:

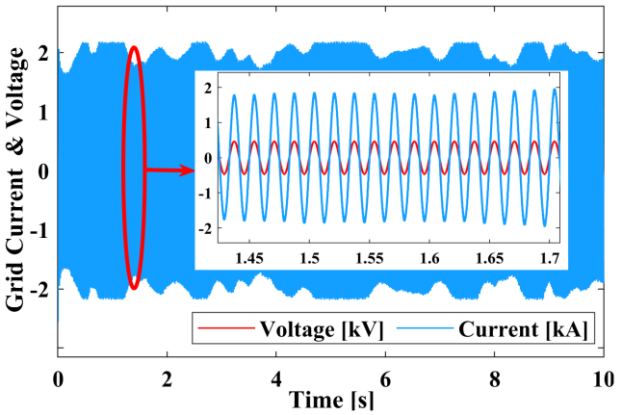


Figure. 13 Grid voltage and current (One phase)

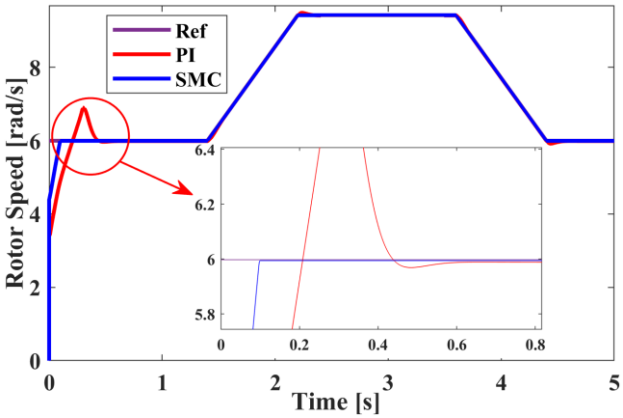


Figure. 14 Generator speed: SMC vs PI

Table1. Parameters of the simulated WT system

| | | | |
|---|---|---|---|
| Rated power | *1.5MW* | Rated wind turbine speed | *1.2 pu* |
| Turbine radius (R) | *36.5* | DC-link voltage | *1150 V* |
| Stator resistance | *1.7 mΩ* | Dc-link Capacitor | *0.023 F* |
| Stator inductance | *0.31 mH* | Line resistance | *0,661 mΩ* |
| PM flux linkage | *2 Wb* | Line inductance | *0,175 mH* |
| Pole pairs | *40* | Grid frequency | *60 Hz* |
| Moment of inertia | *35000* $kg.m^2$ | Grid voltage | *575 V* |

Table 2. Machine side control switching responses

| | SMC | PI |
|---|---|---|
| $V_{dc}$ | *±3V (0.26%)* | *±3.1V (0.26%)* |
| $I_{d1}$ | *±0.03 pu* | *±0.09 pu* |
| $I_{q1}$ | *±0.046 pu* | *±0.1 pu* |
| $I_{d2}$ | *±0.028 pu* | *±0.08 pu* |
| $I_{q2}$ | *±0.031 pu* | *±0.075 pu* |

$$\boldsymbol{\nabla}_{WECS}(\%) = \frac{\int_{\boldsymbol{begin}}^{\boldsymbol{end}} \boldsymbol{P_{injct}dt}}{\int_{\boldsymbol{begin}}^{\boldsymbol{end}} \boldsymbol{P_{opt}dt}} \quad (57)$$

Where, $\boldsymbol{\nabla}_{WECS}$ is the effectiveness ratio of (VSWT) , $\boldsymbol{P_{injct}}$ is the electrical power and $\boldsymbol{P_{opt}}$ is the optimal power which can be calculated using Eq. (7). It can be determined that the WECS effectiveness using the Sliding mode control attains 91,14%, while the PI efficiency is limited to 86,2%. In addition, the difference between the desired speed and the actual speed of the system when the response has reached his steady state is:

$$e_{ss} = 100\%.\lim_{t\to\infty}\big(r - y(t)\big) \quad (58)$$

$(r)$ is the reference and $y(t)$ is the actual value. Therefore, the steady state error of the improved SMC (0.335%) is smaller than the PI (0.87%).

Based on the foregoing, the proposed SMC has demonstrated successfully the capability to enhance the system exploitation and robustness, ensuring its stability, while maintaining the system simplicity. Over and above, the grid side control has shown an excellent active and reactive power flow, according to the needs and necessities of the network.

## 6. Conclusion

In this work, a robust Sliding Mode Control strategy is implemented to control a wind energy conversion system with direct driven large scale five-phase PMSG, connected to the electrical grid. The leading purpose of this study is distributed into two parts with two sliding mode control schemes. First part is to control the machine side converter in order to maximize the extracted power of VSWT (MPPT control) during wind speed variations under its rated value, a pitch angle control is carried out to limit the power extraction above the rated wind speed, so as to guarantee (WT) safety. The second part is to manage the grid supply by maintaining the DC-link voltage at a constant value, and forcing the reactive power to zero value as a means to achieve an active power injection into the grid with Unity Power Factor. The performance of proposed SMC for WECS has been verified and proved during changeable wind speed. (Smooth) function has been used to reduce the level of chattering phenomenon instead of regular signum function. Besides, the system stability using the main approach is confirmed through Lyapunov function. The simulation results of designed SMC show a great accuracy, fast responses and high level of efficiency enhancement from 86,2% to 91,14 %. Furthermore, the steady-state error is negligible. Hence, the improved SMC demonstrates its superiority, and overrides the weaknesses of conventional controllers against the weather condition variations.

The following progress of this effort would include but not limited to the system reliability and efficiency examination in the existence of grid disturbances. Moreover, a comparison with other nonlinear controls such as ANN strategies or enhanced SMC methods as high order SMC is required.

## Conflicts of Interest

The authors declare no conflict of interest.

## Author Contributions

Conceptualization, methodology, software, investigation, validation, writing—original draft preparation, data curation, writing and editing, S.E Rhaili; resources, S.E Rhaili and R. Moutchou; review, S.E Rhaili, S. Marhraoui and N. EL Hichami; supervision, A. Abbou.

| **Abbreviations List** | | | |
|---|---|---|---|
| WECS | Wind Energy Conversion System | MPPT | Maximum power point tracking |
| VSWT | Variable wind turbine | MSC | Machine Side Converter |
| WT | Wind turbine | GSC | Grid Side Converter |
| SMC | Sliding mode control | VOC | Voltage-oriented control |
| PMSG | Permanent magnet synchronous generator | UPF | Unity Power Factor |
| DFIGs | induction generators | PLL | The voltage phase locked loop |
| TSR | Tip speed ratio ($\lambda$) | ANN | Artificial neural networks |

| **Symbols List** | | | |
|---|---|---|---|
| $\rho$ | Air mass density | $L_{d,q}$ | The stator *dq-axis* inductances |
| R | Turbine radius ($m$) | $L_s$ | Stator inductance |
| $S = \pi . R^2$ | Turbine blades swept area ($m^2$) | $V_{d1,d2}$ *and* $V_{q1,q2}$ | The stator *dq-axis* voltages |
| $V_w$ | The wind speed (*m/s*) | $i_{d1,d2}$ *and* $i_{q1,q2}$ | The stator *dq-axis* current components |
| $\beta$ | The blade pitch angle | $V_{gcd}$, $V_{gcq}$ | Grid Side Converter voltage components |
| $\lambda = R.\omega_m/V_w$ | The tip-speed ratio | $V_{gd}$, $V_{gq}$ | Grid voltage components |
| Cp | Power coefficient | $i_{gd}$, $i_{gq}$ | Grid current components |
| $J$ | The Total Moment of inertia | $L_g$ | Inductance of grid filter |
| $B$ | The friction coefficient | $R_g$ | Resistance of grid filter |
| $\omega_m$ | Generator speed | $\omega_g = 2\pi f_g$ | Grid voltages angular frequency |
| $\omega_e$ | Electrical angular velocity | $\psi_{pm}$ | The rotor permanent magnet flux-linkage |
| $P_m$ | Mechanical power | $\delta_n$ | Positive gain of SMC |
| $T_m$ | Mechanical torque | $\delta_{d1}$, $\delta_{q1}$, $\delta_{d2}$, $\delta_{q2}$ | Gains of machine side switching efforts |
| $T_e$ | Electromagnetic torque | $\delta_1$, $\delta_2$ | Gains of grid side switching efforts |
| $P$ | The number of poles | $e_{ss}$ | Steady state error |
| $R_s$ | The stator resistance | | |

## References


[1] B. Beltran, M. E. H. Benbouzid, and T. Ahmed-Ali, "Second-Order Sliding Mode Control of a Doubly Fed Induction Generator Driven Wind Turbine", *IEEE Transactions on Energy Conversion*, Vol. 27, No. 2, pp. 261-269, 2012.

[2] S. Sharma and B. Singh, "Control of Permanent Magnet Synchronous Generator-Based Stand-Alone Wind Energy Conversion System", *IET Power Electronics*, Vol. 5, No. 8, pp. 1519-1526, 2012.

[3] M. Chinchilla, S. Arnaltes, and J. C. Burgos, "Control of Permanent-Magnet Generators Applied to Variable-Speed Wind-Energy Systems Connected to The Grid", *IEEE Transactions on Energy Conversion*, Vol. 21, No. 1, pp. 130-135, 2006.

[4] S. Rhaili, A. Abbou, S. Marhraoui, and N. El Hichami, "Vector Control of Five-Phase Permanent Magnet Synchronous Generator Based Variable-Speed Wind Turbine", In: *Proc. of International Conf. on Wireless Technologies, Embedded and Intelligent Systems*, pp. 1-6, 2017.

[5] H. H. H. Mousa, A. R. Youssef, and E. E. M. Mohamed, "Optimal Power Extraction Control Schemes for Five-Phase PMSG Based Wind Generation Systems", *Engineering Science and Technology, an International Journal*, Vol. 23, No. 1, pp.144–155, 2020.

[6] G. Michalke, A. D. Hansen, and T. Hartkopf, "Control Strategy of a Variable Speed Wind Turbine with Multipole Permanent Magnet Synchronous Generator", In: *Proc. of Eur. Wind Energy Conf. Exhib*, Milan, pp.705–710, 2007.

[7] V. Oghafy and H. Nikkhajoei, "Maximum Power Extraction for A Wind-Turbine Generator with No Wind Speed Sensor", In: *Proc. of the IEEE Power and Energy Society General Meeting - Conversion and Delivery of Electrical Energy in the 21st Century*, pp. 1-6, 2008.

[8] N. A. Orlando, M. Liserre, R. A. Mastromauro, and A. Dell'Aquila, "A Survey of Control Issues In PMSG-Based Small Wind-Turbine Systems", *IEEE Transactions on Industrial Informatics*, Vol. 9, No. 3, pp. 1211-1221, 2013.

[9] L. A. Soriano, W. Yu, and J. D. J. Rubio, "Modeling and Control of Wind Turbine", *Mathematical Problems in Engineering*, Vol. 2013, Article ID 982597, 2013.

[10] S. Rhaili, A. Abbou, S. Marhraoui, N. El Hichami, and A.V. Hemeyine, "Robustness Investigation of Vector Control of Five-Phase PMSG Based Variable-Speed Wind Turbine under Faulty Condition", In: *Proc. of The IEEE International Conf. on Renewable Energies,*

*Power Systems & Green Inclusive Economy*, Casablanca, pp. 1-6, 2018.

[11] Y. Errami, M. Maaroufi, and M. Ouassaid, "A MPPT Vector Control of Electric Network Connected Wind Energy Conversion System Employing PM Synchronous Generator", In: *Proc. of International Renewable and Sustainable Energy Conf.*, pp. 228-233, 2013.

[12] Y. Errami, M. Maaroufi, M. Cherkaoui, and M. Ouassaid, "Maximum Power Point Tracking Strategy and Direct Torque Control of Permanent Magnet Synchronous Generator Wind Farm", In: *Proc. of IEEE International Conf. on Complex Systems*, pp. 1-6, 2012.

[13] N. El Ouanjli, A. Derouich, A. Chebabhi, and M. Taoussi, "A Comparative Study Between FOC and DTC Control of the Doubly Fed Induction Motor (DFIM)", In: *Proc. of International Conf. on Electrical and Information Technologies*, Rabat, pp. 1-6, 2017.

[14] S. Dwivedi and B. Singh, "Vector Control vs Direct Torque Control comparative evaluation for PMSM drive", In: *Proc. of Joint International Conf. on Power Electronics, Drives and Energy Systems*, pp. 1-8, 2010.

[15] H. Vahedi, A. Sheikholeslami, M.T Bina, and M. Vahedi, "Review and Simulation of Fixed and Adaptive Hysteresis Current Control Considering Switching Losses and High-Frequency Harmonics", *Advances in Power Electronics*, Vol. 11, ID 397872, 2011.

[16] N. T. Vu, H. H. Choi, and J. Jung, "Certainty Equivalence Adaptive Speed Controller for Permanent Magnet Synchronous Motor", *Mechatronics*, Vol. 22, No. 6, pp. 811–818, 2012.

[17] Q. Wang, H. Yu, M. Wang, and X. Qi, "A Novel Adaptive Neuro-Control Approach for Permanent Magnet Synchronous Motor Speed Control", *Energies*, Vol. 11, No. 9, 2018.

[18] Y. El Mourabit, A. Derouich, A. El Ghzizal, N. El Ouanjli, and O. Zamzoum, "Nonlinear backstepping control for PMSG wind turbine used on the real wind profile of the Dakhla-Morocco city", *Int. Trans. Electr. Energ. Syst.*, Vol. 30, No. 4, e12297, 2020.

[19] S. Rhaili, A. Abbou, A. Ziouh, and R. Elidrissi, "Comparative Study between PI and FUZZY Logic Controller in Vector Controlled Five-Phase PMSG Based Variable-Speed Wind Turbine", In: *Proc. of IEEE 12th International Conf. on Compatibility, Power Electronics and Power Engineering*, Doha, Qatar, pp. 1-6, 2018.

[20] S. E. Rhaili, A. Abbou, N.E. Hichami, and S. Marhraoui, "A New Strategy Based Neural Networks MPPT Controller for Five-phase PMSG Based Variable-Speed Wind Turbine", In: *Proc. of the 7th International Conf. on Renewable Energy Research and Applications*, Paris, France, pp. 1038-1043, 2018.

[21] V. Utkin, J. Guldner, and J. Shi, *Sliding Mode Control in Electro-Mechanical Systems, 2nd ed.*, CRC Press, Boca Raton, F.L. 2009.

[22] A. A. Z. Diab, A. A. Ahmed, and H. A. Abdelsalam, "Fuzzy-based Adaptive Sliding Mode Control for a Direct-Driven PMSG Wind Energy System", In: *Proc. of the 21st International Middle East Power Systems Conf.*, Cairo, pp. 81-88, 2019.

[23] Y. Zafari, A. H. Mazinan, and S. Shoja-Majidabad, "Speed control of Five-Phase IPMSM through PI, SMC and FITSMC Approaches Under Normal and Open Phase Faulty Conditions", *Automatika*, Vol. 58, No. 4, pp. 506-519, 2017.

[24] H. H. H. Mousa, A. Youssef, and E. E. M. Mohamed, "Model Predictive Speed Control of Five-Phase PMSG Based Variable Speed Wind Generation System", In: *Proc. of the Twentieth International Middle East Power Systems Conf.*, Cairo, pp. 304-309, 2018.

[25] S. Tripathi, A. Tiwari, and D. Singh, "Grid-Integrated Permanent Magnet Synchronous Generator Based Wind Energy Conversion Systems: A Technology Review", *Renewable and Sustainable Energy Reviews*, Vol. 51, pp. 1288-1305, 2015.

[26] B. Boukezzar and M. M'Saad, "Robust Sliding Mode Control of a DFIG Variable Speed Wind Turbine for Power Production Optimization", In: *Proc. of the 16th Mediterranean Conf. on Control and Automation*, pp. 795-800, 2008.

[27] P. Gajewski, and K. Pieńkowski, "Analysis of Sliding Mode Control of variable speed wind turbine system with PMSG", In: *Proc. of International Symposium on Electrical Machines*, Naleczow, Poland, pp. 1-6, 2017.

[28] G. Zhuo, J. Hostettler, P. Gu, and X. Wang, "Robust Sliding Mode Control of Permanent Magnet Synchronous Generator-Based Wind Energy Conversion Systems", *Sustainability, MDPI, Open Access Journal*, Vol. 8, No. 12, pp. 1-20, 2016.

[29] H. Athari, M. Niroomand, and M. Ataei, "Review and classification of control systems in grid-tied inverters", *Renewable and Sustainable Energy Reviews*, Vol. 72, pp. 1167-1176, 2017.